Native CRISPR-Cas mediated in situ genome editing reveals extensive resistance synergy in the clinical multidrug resistant *Pseudomonas aeruginosa*

Zeling Xu,[a] Ming Li,[b] Yanran Li,[a] Huiluo Cao, [b]* Hua Xiang, [b]# Aixin Yan [a]#

[a]School of Biological Sciences, The University of Hong Kong, Hong Kong SAR, China

[b]State Key Laboratory of Microbial Resources, Institute of Microbiology, Chinese Academy of Sciences, Beijing, China

Running head: Harnessing CRISPR to tackle antibiotic resistance

#Address correspondence to Hua Xiang, xiangh@im.ac.cn or Aixin Yan, ayan8@hku.hk

*Present address: Department of Microbiology, Li Ka Shing Faculty of Medicine, The University of Hong Kong, Hong Kong SAR, China.

Z.X. and M.L. contributed equally to this work.

Word counts: abstract (250); text (5157)

ABSTRACT

Antimicrobial resistance (AMR) is imposing a global public health threat. Despite its importance, characterizing drug resistance directly in the clinical isolates of resistant pathogens is frequently hindered by the lack of genome editing tools in these "non-model" strains. *Pseudomonas aeruginosa* is both a prototypical multidrug resistant (MDR) pathogen and a model species for CRISPR-Cas research. In this study, we report the successful development of a simple and efficient one-plasmid mediated, one-step genome editing approach in a paradigmatic MDR strain PA154197 by exploiting its native type I-F CRISPR-Cas system. The technique is readily applicable in two additional type I-F CRISPR-containing, clinical and environmental *P. aeruginosa* isolates. A two-step In-Del strategy involving insertion and subsequent deletion of a tag nearby the desired editing site is further developed to edit the genomic locus lacking an effective PAM (protospacer adjacent motif) or within an essential gene, which principally allows any non-lethal genomic manipulation in the strains. With these powerful techniques, the resistant determinants of PA154197 were delineated in its native genetic background. Moreover, relative contributions and extensive synergy of different resistance determinants previously unrecognized by using laboratory strains were disclosed. The two efflux pumps with different substrate preference, MexAB-OprM and MexEF-OprN, synergistically expel fluoroquinolones, trimethoprim and chloramphenicol. Among the three resistant mutations synergizing fluoroquinolones resistance, *gyrA* mutations elicit a greater resistance than drug efflux by MexAB-OprM or MexEF-OprN. These results advanced our understanding of the MDR development of clinical *P. aeruginosa* strains and demonstrated the great potentials of native CRISPR systems in AMR research.

IMPORTANCE

Genome editing and manipulation often revolutionizes the understanding, exploitation, and control of microbial species. Despite the presence of well-established genetic manipulation tools in various model strains, their applicability in the medically, environmentally, and industrially significant, "non-model" strains is often hampered owing to the vast diversity of DNA homeostasis in these strains and the cytotoxicity of the heterologous CRISPR-Cas9/Cpf1 system. Harnessing the native CRISPR-Cas systems broadly distributed in prokaryotes with built-in genome targeting activity presents a promising and effective approach to resolve these obstacles. We explored and exploited this methodology in the prototypical multidrug resistant pathogen *P. aeruginosa* by exploiting the most common subtype of the native CRISPR systems in the species. Our successful development of the first type I-F CRISPR-mediated genome editing technique and its subsequent extension to additional clinical and environmental *P. aeruginosa* isolates opened a new avenue to the functional genomics of antimicrobial resistance in pathogens.

KEYWORDS: Multidrug resistance, *Pseudomonas aeruginosa*, Native CRISPR-Cas system, Multidrug efflux pump, Resistance synergy

INTRODUCTION

Antimicrobial resistance (AMR) is imposing an alarming threat to the global public health. Of particular challenging in clinics are those "ESKAPE" pathogens which are extraordinary to engender antibiotic resistance, i.e. *Enterococcus spp.*, *Staphylococcus aureus*, *Klebsiella spp.*, *Acinetobacter baumannii*, *Pseudomonas aeruginosa*, and *Enterobacter spp.*. Owing to its intrinsic resistance to a variety of antimicrobials and the enormous capacity of developing acquired

resistance during antibiotics chemotherapies, *Pseudomonas aeruginosa* is recognized as the prototypical multidrug resistant (MDR) pathogen (1-4). Remarkably, in recent years, international high-risk clones of MDR *P. aeruginosa* have emerged and have been shown to cause worldwide outbreaks (5). Genetic analyses reveal that these clones often contain a complex set of resistance markers (6-8) including both the genetic variations that lead to resistance to specific classes of antibiotics, such as mutations in drug targets and acquisition of drug inactivation enzymes, and those conferring simultaneous resistance to multiple drugs, such as over-expression of multidrug efflux pumps. However, whether the genetic mutations identified by comparative genomics indeed contribute to the resistance phenotypes remains to be verified in the native genetic backgrounds of the strains. Furthermore, the relative contributions and the interplay of the different resistance determinants in shaping the MDR profile of the clinically significant resistant pathogens remain largely elusive.

Current knowledge of the resistance determinants and their mechanisms are obtained largely by reconstitution of the identified genetic variations or over-expressing multidrug efflux pumps in laboratory model strains (9, 10). Several studies indicated that no obvious multiplicative or synergetic effects were observed between over-expression of multidrug efflux pumps and the mechanisms causing resistance to specific classes of antibiotics, such as over-expression of the cephalosporinase AmpC and mutations in the DNA gyrase GyrA or topoisomerase IV ParC (11-14). It was proposed that synergistic interactions occur when different types of multidrug efflux systems operate simultaneously, i.e. the tripartite resistance-nodulation-division (RND) efflux pumps and the single component pump (e.g. TetA/C) (15). However, it is increasingly recognized that the genetic background of the resistant strains and epistasis among different resistant mutations play an important role in shaping the resistance profile of the clinical strains (16-18).

Hence, it is necessary to verify the functions of identified resistant mutations in the native genetic background of the clinical MDR strains. The major obstacle of these molecular characterizations is the lack of efficient and readily applicable genomic editing tools in these "non-model" strains. In addition to be a prototypical MDR pathogen, *P. aeruginosa* is an important model system for CRISPR-Cas research, especially the type I CRISPR-Cas system. Phylogenetic analysis revealed that CRISPR-Cas systems are widely distributed in global AMR *P. aeruginosa* isolates with more than 90% belonging to the I-E or I-F subtypes (19). Owing to its built-in genome targeting activity and reprogrammable feature, in recent years, repurposing the native CRISPR-Cas systems which are present in the vast number of prokaryotic genomes for genetic editing is emerging as an increasingly compelling strategy especially in those species with low transformation efficiency and poor homologous recombination. For instance, the native type I-B CRISPR-Cas system in *C. tyrobutyricum*, *C. pasteurianum*, *H. hispanica* (archaea) and the type I-A & III-B native CRISPR-Cas systems in *S. islandicus* (archaea) have been successfully harnessed for genome editing in the corresponding species recently (20-23). Whether the broadly distributed native CRISPR-Cas systems in *P. aeruginosa*, especially the most common subtype of I-F, can be harnessed for genome editing and functional genomics of antimicrobial resistance remains unexplored.

Previously, we have isolated a MDR *P. aeruginosa* strain PA154197 which displays high epidemic potentials with a resistance profile (resistant to five of the seven commonly used antipseudomonal drugs) comparable to the international high-risk clone ST175 (24). A large number of resistant mutations were predicted by genomic analysis, including mutations in the DNA gyrase *gyrA* and Cephalosporinase *ampC* which are associated with resistance to fluoroquinolones and β-lactams (25, 26), respectively, and gene mutations causing over-production of three multidrug efflux pumps MexAB, MexEF, and MexGHI (Table S1). Sequencing data reveal that PA154197 contains

a native type I-F CRISPR-Cas locus in its genome. These together make PA154197 a paradigm to establish a genome editing approach by exploiting its native CRISPR-Cas system and exploit the system for AMR characterization in the native genetic background of a clinical MDR isolate.

We successfully developed a single plasmid-mediated, one-step precise genomic manipulation technique in PA154197 by exploiting its native type I-F CRISPR-Cas system, and a two-step In-Del approach to edit the genomic loci lacking an effective PAM (protospacer adjacent motif) sequence. Exploiting this efficient technique, we revealed the key resistant determinants and the extensive synergy of different resistance mechanisms in shaping the MDR of PA154197 which were unrecognized by investigations in the laboratory strains. Moreover, the established genome editing system can be readily applied to two additional type I-F CRISPR-containing, clinical and environmental *P. aeruginosa* strains PA150567 and Ocean-100. These results demonstrated the general applicability of native CRISPR-based editing system in the characterization of resistance development of clinical MDR *P. aeruginosa* isolates, and presumably other species.

RESULTS

PA154197 contains a functional type I-F CRISPR-Cas system.

Analysing the native CRISPR-Cas loci in PA154197 identified the type I-F signature genes *cas8f*, *cas6f* and the unique *cas2-cas3* fusion of the system (Fig. 1A) (27). The *cas* operon of the system is found to be sandwiched by two convergent CRISPRs. Their consensus repeat sequence differs by only one nucleotide, and their spacers are nearly identical in size (32 bp). In addition, a number of spacers show significant homology to phage or putative prophage sequences (data not shown), suggesting the DNA interference potential of this system and the feasibility of exploiting this system for genome editing.

To harness the native CRISPR-Cas for genome editing, we first tested the genome targeting activity of the system. We selected *mexB* gene as the target gene for this purpose, which encodes the inner membrane component of the housekeeping efflux system MexAB-OprM. Previous studies revealed that the canonical target of the type I-F CRISPR-Cas system is 5'-CC-protospacer-3' (28) (note that our study follows the standard guide-centric PAM definition (29)). Hence, an internal 32-bp sequence preceded by a 5'-CC-3' PAM in *mexB* is selected as the target (PAM-protospacer). The 32-bp spacer flanked by 28-bp repeat sequences at both ends, termed as a mini-CRISPR, is then cloned into the pMS402 vector, which contains a kanamycin-resistant gene and a *lux* reporter cassette (30), to generate the targeting plasmid pAY5233 (Fig. 1B). To ensure its expression and efficient targeting, a strong promoter P*tat* (31) is selected to drive the expression of the mini-CRISPR. To overcome the poor antibiotics-based selection of transformants in MDR strains, the P*tat*-mini-CRISPR is cloned upstream of the *lux* operon in pMS402 in frame such that P*tat* simultaneously drives the expression of the CRISPR element and the *lux* operon which assists transformant screening (Fig. 1B). When pAY5233 and the control plasmid pAY5211 (which contains all the elements described above except the mini-CRISPR fragment) were introduced into PA154197 cells, a dramatic decrease of the transformants recovery was observed comparing to the non-targeting control (Fig. 1C), implying the occurrence of the detrimental chromosome cleavage in the cell. This result confirms that the native CRISPR-Cas system is active in PA154197.

Harnessing the native type I-F CRISPR-Cas system to delete the resistance gene *mexB*.

To exploit the system for gene deletion (Δ*mexB* as an example), we then assembled a 1-kb donor sequence consisting of the 500-bp upstream and 500-bp downstream of *mexB* for homologous recombination, and inserted it into pAY5233 to yield pAY5235, termed as the editing plasmid (Fig.

157 1D). The number of transformants of pAY5235 is significantly increased (by more than 10-fold)
158 compared to pAY5233 (Fig. 1C), suggesting the occurrence of homologous recombination by the
159 provision of the donor sequence. We randomly selected eight luminescence positive colonies for
160 colony PCR and DNA sequencing validation and found four colonies showed the desired, scarless
161 and precise deletion of *mexB* in the chromosome (Fig. 1E and 1F). These results demonstrate the
162 success of genome editing by exploitation of the native type I-F CRISPR-Cas system in the clinical
163 MDR isolate PA154197 by one-step introduction of a single editing plasmid.
164 The success rate of 4/8 seemed moderate. However, we speculate that it was due to the unusually
165 large size (3141 bp) of *mexB* rather than the efficiency of the editing technique, as subsequent
166 attempts to delete shorter fragments, i.e. 50-bp, 500-bp, or 1000-bp deletion within *mexB* (Fig.
167 S1A), yielded significantly improved success rate, i.e. 8/8 (50-bp deletion), 7/8 (500-bp deletion),
168 and 7/8 (1000-bp deletion) (Fig. S1B). Hence, the native CRISPR-based editing strategy we
169 developed is efficient to knock out a target gene, since the average gene length in prokaryotes is
170 ~1 kb (32). Indeed, the 4/8 successful rate for the 3-kb *mexB* is fairly high according to several
171 recent reports (33, 34). Moreover, we found the editing plasmid can be readily cured following
172 culturing the edited cells in the absence of the antibiotic (kanamycin) pressure overnight (Fig. S2),
173 suggesting the feasibility of multiple rounds of gene editing using the reprogrammable pAY5235
174 editing platform.
175 To examine the applicability of the technique in other type I-F CRISPR-Cas containing *P.*
176 *aeruginosa* strains, we set out to construct *mexB* deletion in a carbapenem resistant clinical strain
177 PA150567 (accession number: LSQQ00000000) isolated from the Queen Mary Hospital, Hong
178 Kong and an environmental strain Ocean-100 (accession number: NMRS00000000) isolated from
179 the North Pacific Ocean (35). As expected, transformation of the targeting plasmid pAY5233 led

to DNA interference in the two strains, and the editing plasmid pAY5235 achieved the desired *mexB* deletion with comparable successful rate as in PA154197 (Fig. S3), confirming the general applicability of the developed editing system in clinically and environmentally isolated, "non-model" *P. aeruginosa* strains.

Over-expression of the MexAB-OprM and MexEF-OprN efflux pumps contributes significantly to the MDR of PA154197.

Three multidrug efflux pumps MexAB-OprM, MexEF-OprN, MexGHI-OpmD were found to be hyper-expressed in PA154197 compared to PAO1 (24). To test their contribution to the resistance phenotype of the MDR strain, we first deleted *mexB*, *mexF*, and *mexH*, which encodes the inner membrane channel of the three efflux systems, respectively. We found that except for IPM, Δ*mexB* leads to significant decrease in the MICs of all five classes of common antipseudomonal antibiotics PA154197 is resistant to (Table 1), i.e. ATM (64 to 1), CAZ (16 to 2), TZP (32 to 0.5), MEM (4 to <0.125), CAR (>128 to 1), LVX (32 to 16), and CIP (16 to 8), with a greater effect on the antipseudomonal β-lactams (CAR,, CAZ, MEM, ATM), and penicillin-β-lactamase inhibitor combinations (TZP) than on fluoroquinolones (LVX and CIP). Δ*mexF* leads to the decrease in MICs of antipseudomonal fluoroquinolones, i.e. LVX (32 to 16) and CIP (16 to 4), consistent with the previous report of the substrate profile of the pump using *mexEF-oprN* over-expression construct in PAO1 (36). Double deletion of *mexB* and *mexF* leads to dramatic decrease in MICs of all antipseudomonal antibiotics (except IPM) (Table 1) and several other antimicrobial agents tested (Table 2), suggesting that hyper-active drug efflux by these two pumps contributes significantly to the MDR profile of PA154197. Moreover, different from the observations obtained by over-expressing several *P. aeruginosa* efflux pumps in *E. coli* (15), significant synergy is

observed between the two tripartite efflux pumps in expelling their common substrates fluoroquinolones as evidenced by the MIC fold change in the Δ*mexB* Δ*mexF* double deletion strain (32-fold) relative to that in single deletion strain (2-fold decrease for LVX in both Δ*mexB* and Δ*mexF*, and 2- and 4-fold decrease for CIP in Δ*mexB* and Δ*mexF*, respectively). Disk diffusion test showed similar susceptibility changes in these strains (Fig. S4). Analysis of the growth curves of these strains in the absence of antibiotics suggested that the observed MIC alterations were not due to intrinsic disadvantages or defects in growth (Fig. S5). Unexpectedly, deletion of another efflux gene *mexH* which is also hyper-expressed in PA154197 (~40-fold higher than in PAO1) (24) did not lead to any detectable difference in the MICs of all the antibiotics and antimicrobial agents tested (Table 1 and 2), suggesting that it does not contribute to the antibiotic resistance of PA154197.

A G226T point mutation in *mexR* is responsible for the *mexAB-oprM* over-expression.

Over-expression of efflux genes is often caused by mutations in their transcription regulators. Comparative genomic analysis revealed a single nucleotide substitution G226T (corresponding to introducing a stop codon at E76) in PA154197 *mexR* compared to that in PAO1 (Fig. S6A). MexR is a transcription repressor of *mexAB-oprM* genes (Fig. 2A) and mutations or pre-mature termination of the protein often leads to over-production of the MexAB-OprM pump and MDR in the cells (37-39). To investigate whether this mutation accounts for the over-expression of *mexAB-oprM*, we reprogramed the editing plasmid pAY5235 by replacing the mini-CRISPR and the donor sequences for *mexB* deletion with those for point mutation of *mexR*, respectively, and constructed the reverse mutation, i.e. T226G in *mexR*. Such editing results in the replacement of *mexR* gene in PA154197 with that from PAO1, hence, the resulting construct is designated as $mexR^{PAO1}$. RT-

qPCR analysis revealed that the transcriptional level of *mexAB* genes in the *mexR*^{PAO1} mutant is significantly reduced comparing with that in the wild-type PA154197, to a level that is similar in PAO1 (Fig. 2B and 2C), suggesting that the G226T mutation in *mexR* is responsible for the over-expression of *mexAB-oprM*. Both MIC analysis and disk diffusion test confirmed that the antibiotics susceptibility profile is similar between the *mexR*^{PAO1} and Δ*mexB* cells (Table 1 and 2, Fig. S4).

An advanced two-step In-Del strategy to edit *mexT* verifies its role in *mexEF* over-expression and repression of *oprD*.

The *mexT* gene encodes a transcription regulator of the *mexEF-oprN* efflux system (Fig. 2A) (9). Our comparative genomic analysis identified an 8-bp deletion in the PA154197 *mexT* compared to PAO1 *mexT* (24). Notably, PAO1 belongs to the "type II" wild type *P. aeruginosa* strains in which MexT is produced as an intrinsically inactive, out-of-frame variant (Fig. S6B) (40). The 8-bp deletion in PA154197 *mexT* principally enables the protein to be translated in-frame and produced as an active MexT transcription activator (40, 41). To verify this in the MDR strain PA154197, we attempted to construct the 8-bp insertion reverse mutation. However, the construction using the same one-step strategy for gene deletion and point mutation described above was not successful. Analysing the DNA sequence of the PAM-protospacer selected for the 8-bp insertion reveals the presence of two 6-bp repeats, which potentially obscures the recognition of the PAM and the subsequent DNA interference (Fig. S7).

To overcome this limitation, we devised a two-step Insert-Delete (In-Del) strategy to achieve editing in these inefficiently targeted sites (Fig. 3A). The approach bypasses the poorly targeted PAM-protospacer by exploiting a proximal auxiliary PAM (152-bp downstream of the desired 8-

bp insertion site) which can be targeted efficiently to firstly insert a 32-bp short tag (5'-TACAACAAGGACGACGACGACAAGGTGATCAG-3') between the PAM and the protospacer. Insertion of the desired 8-bp is subsequently achieved in the second round of editing by exploiting the same PAM but a different protospacer sequence (termed as the PAM-tag-protospacer) and the provision of a donor sequence which lacks the tag sequence but includes the desired insertion sequence, allowing simultaneous removal of the tag and introduction of the desired mutation (Fig. 3A). The success rate for the first and second round editing is found to be 8/8 and 5/8 (Fig. 3B and 3C). This result demonstrates the success of our In-Del strategy, which principally allows genetic manipulations regardless of PAM limitation.

The resulting mutant is designated as *mexT*^{PAO1}. RT-qPCR analysis revealed that transcription level of the *mexEF* genes in the *mexT*^{PAO1} cells is reduced to a level that is similar in PAO1 (Fig. 2D and 2E), suggesting that absence of 8-bp in *mexT* causes over-expression of *mexEF-oprN* in PA154197. Both MIC analysis and disk diffusion test confirmed that the antibiotics susceptibility profile is similar between the *mexT*^{PAO1} and Δ*mexF* cells (Table 1 and 2, Fig. S4). Notably, in addition to activate *mexEF-oprN*, MexT is also known to repress the expression of *oprD* (Fig. 2A), which encodes an important porin protein facilitating the diffusion of carbapenems antibiotics (especially IPM) (42). Hence, a reduced OprD production is frequently linked to increased tolerance to IPM resistance (43) which is observed in PA154197. We next conducted RT-qPCR analysis and found that the transcriptional level of *oprD* in the *mexT*^{PAO1} cells is 3-fold higher than in the PA154197 parent, to a level that is similar in PAO1 (Fig. 2D and 2E). MIC and disk diffusion assays show increased susceptibility of *mexT*^{PAO1} to IPM than the PA154197 parent (Table 1, Fig. S4). Together, these results indicate that the 8-bp deletion in *mexT* contributes to the resistance of PA154197 to fluoroquinolones and increased tolerance to IPM (breaking point of IPM is 4) by

simultaneously up-regulating the expression of *mexEF-oprN* and down-regulating the expression of *oprD*.

Mutations in the essential gene *gyrA* constitutes another fluoroquinolone resistance determinant in PA154197.

Although Δ*mexB* Δ*mexF* led to a dramatic decrease (32-fold) in MICs of the fluoroquinolones LVX (32 to 1) and CIP (16 to 0.5), the MIC values of the two antibiotics are still higher than that in PAO1 (both are 0.25), suggesting the presence of additional fluoroquinolone resistance determinants in PA154197. Two genetic variations in the DNA gyrase gene *gyrA* are identified in PA154197: the well-studied T248C substitution (corresponding to T83I) in the quinolone resistance determining region (QRDR) which abolishes (fluoro)quinolone binding (44), and a new genetic variation of 6-bp deletion (^{2723}CCGAGT^{2728}) in the C-terminal domain (CTD) of GyrA which is reported to fine-tune the ATP turnover and DNA supercoiling activity of the gyrase (45) (Fig. S6C). To investigate whether these genetic variations contribute to fluoroquinolone resistance, we employed the two-step In-Del strategy described above to replace the essential gene *gyrA* in PA154197 with that from PAO1, generating *gyrA*^{PAO1} (Fig. S8). MIC analysis and disk diffusion assay showed that this gene replacement leads to 8- and 4-fold decrease in the MICs of LVX and CIP, respectively (Table 1), suggesting that the genetic variations in *gyrA* also play a significant role in the fluoroquinolone resistance in PA154197. The fact that the MICs fold change in *gyrA*^{PAO1} relative to its PA154197 parent is consistent with that when the single T83I substitution is introduced into the laboratory strain PA14 (10) indicates that the contribution of *gyrA* mutation to the fluoroquinolone resistance of PA154197 is mainly due to the T83I substitution.

Extensive synergy of different resistant mutations are present in PA154197.

Previous investigations of the antibiotic resistance determinants and the substrate profile of multidrug efflux pumps in the laboratory model strains (10, 36) is often incapable of revealing the relative contribution and synergy of multiple, different resistance determinants owing to its susceptible strain background. To explore this, we constructed a series of single, double and triple mutations using the efficient editing technique developed and examined the relative contributions and interplay of the identified resistance determinants in PA154197. As shown in Table 1, single deletion of *mexB*, *mexF*, or replacement of the *gyrA* gene with that of PAO1 (*gyrA* ^{PAO1}) led to a decrease of the LVX MIC to 1/2, 1/2, and 1/16 of the WT, and the CIP MIC to 1/2, 1/4, and 1/4 of the WT, respectively (Table 1), suggesting that mutations in *gyrA* play a greater role in causing fluoroquinolone resistance than the drug efflux by MexAB-OprM or MexEF-OprN. Inactivation of all three determinants (*gyrA*^{PAO1} *mexR*^{PAO1} *mexT*^{PAO1} strain) leads to the complete loss of resistance to LVX and CIP (MIC being 1/128 of the WT), confirming that the three resistance determinants synergizing fluoroquinolone resistance in PA154197. Interestingly, in the case of another quinolone antimicrobial agent nalidixic acid, single or double interference of *mexB* (*mexR*^{PAO1}), *mexF* (*mexT*^{PAO1}), and *gyrA* (*gyrA*^{PAO1}) has no effect on the resistance to this agent, and only simultaneous interference of all three determinants leads to the decrease of MIC to 1/4 of the WT, suggesting that these three genetic variations cooperates NAL resistance.

Our investigations above have demonstrated the synergy of MexAB-OprM and MexEF-OprN in expelling their common substrates of fluoroquinolones LVX and CIP. To further examine the substrates of these two efflux pumps and their interplay in expelling antimicrobials, the MIC alterations of several other antibiotics and antimicrobial agents are examined (Table 2). In addition

318 to LVX and CIP, we observed obvious synergy of the two pumps in the extrusion of trimethoprim
319 (TMP) and chloramphenicol (CHL). Combining the MIC alterations in the Δ*mexB*, Δ*mexF* and
320 Δ*mexB* Δ*mexF* presented in Table 1 and 2, a rather complete substrates profile of the two efflux
321 pumps with relative substrates preference is mapped (Fig. 4). This information enriched our
322 understanding of the relative contributions of resistance determinants and their interplay in
323 clinically isolated MDR strains using PA154197 as a paradigm.
324

325 **DISCUSSION**

326 Emergence of resistance to multiple antimicrobial agents in pathogenic bacteria has become a
327 significant global public health threat as there are fewer, or even sometimes no, effective
328 antimicrobial agents to treat the infections caused by these bacteria. The MDR/XDR international
329 high-risk clones of *P. aeruginosa* are especially challenging in therapeutics owing to their
330 extraordinary drug resistance and rapid dissemination in hospitals worldwide (46-48). Previous
331 molecular epidemic analyses have largely focused on identification of genetic variations in the
332 resistant isolates in comparison with the model strain PAO1 (49). To our knowledge, there has
333 been no systematic, targeted molecular investigations of resistance development characterized
334 directly in the native genetic background of clinical MDR isolates. In this study, we report the first
335 single-plasmid-mediated, one-step genome editing technique directly applicable in the native
336 CRISPR-Cas containing, clinical *P. aeruginosa* strains, and its exploitation in AMR
337 characterization which provided new insight into the contribution and interplay of resistant
338 mutations in shaping the clinically significant MDR.
339 In comparison with a recently reported heterologous Cas9-based genome editing method which
340 requires successive transformation of two editing plasmids (33), and the conventional two-step

allelic exchange method (50) which takes more than two weeks to construct a mutant with an undesirable FLP site permanently remained in the edited site, our method using a single plasmid to achieve editing in one-step represents a more efficient and clean genome editing method which can be completed within one week, i.e. 3-4 days for constructing the editing plasmid and 2-3 days for the luminescence-assisted selection and verification. The two-step In-Del strategy further developed to circumvent the limitation of poorly targeted genomic loci principally allows us to conduct any non-lethal genetic manipulation in the bacterial genome (Fig. 5), greatly expanding and accelerating the molecular characterizations of the CRISPR-containing, MDR *P. aeruginosa* isolates. The methodology should be readily extended to other clinically significant pathogens, such as *Acinetobacter baumannii* and *Klebsiella spp*. to facilitate resistance characterization and interference in these species.

Employing this powerful and efficient genome editing methodology, we not only verified the previously proposed resistant mechanisms but also revealed the interplay of different resistant determinants previously unrecognized by investigations in model strains. The G226T substitution in *mexR* is a newly identified point mutation occurred in PA154197 that leads to the de-repression of *mexAB-oprM*. Three resistant mutations are found to synergize fluoroquinolone resistance, and mutations in *gyrA* elicit a greater extent of resistance than over-production of MexAB-OprM or MexEF-OprN. We speculate that mutations leading to over-production of MexAB-OprM and MexEF-OprN proceed the *gyrA* mutations in PA154197 as it has been documented that drug efflux not only directly causes antibiotic resistance by expelling structurally diverse antibiotics but also drives the acquisition of additional resistance mechanisms by lowering intracellular antibiotic concentration and promoting mutation accumulation (14, 51). Repression of MexAB-OprM and MexEF-OprN efflux systems, de-repressing the expression of the porin OrpD, combined with

reverse mutations in *gyrA* literally converted the MDR clinical strain PA154197 to a susceptible strain (*gyrA* ^{PAO1} *mexR*^{PAO1} *mexT*^{PAO1}), confirming the key roles these resistance determinants play in shaping MDR in PA154197. Lastly, we dissected substrates profile and preference of the MexAB-OprM and MexEF-OprN efflux pumps and revealed the obvious synergy of the two pumps in expelling of fluoroquinolones, trimethoprim, and chloramphenicol. Notably, studies carried out in a susceptible reference *P. aeruginosa* strain and in *E. coli* showed no synergy between MexAB-OprM and MexEF-OprN in expelling fluoroquinolones (10, 15). This discrepancy may be due to the different genetic background of the strains used which underlie the importance of investigating resistance development in the native genetic background of resistant isolates.

Although genome sequencing and comparative genomics can identify the genetic variations in resistance genes, whether and to what extent these variations contribute to the resistance phenotype cannot be disclosed merely by genomic and transcriptome analyses. For instance, we found that over-expression (~40 fold higher than in PAO1) of the efflux gene *mexH* and nucleotide substitution in *parS* does not contribute to the drug resistance in PA154197 (Table 1 and 2). These results suggest that not all genetic variations identified in resistance genes lead to the development of antibiotic resistance, further highlighting the importance of the targeted functional genomics investigations directly in the clinically isolated resistant strains.

MATERIAL AND METHODS

Bacterial strains, culture conditions.

All the bacterial strains used and constructed in this study are listed in Table S2. *E. coli* DH5α is used for plasmid construction and is usually cultured at 37°C in Luria-Bertani (LB) broth or on the

LB agar plate supplemented with 20 μg/ml Kanamycin (KAN). *P. aeruginosa* PA154197 was isolated from the Queen Mary Hospital in Hong Kong, China (24). PA154197 and its derivatives were selected in LB (broth or agar) with 500 μg/ml KAN at 37°C.

Plasmid construction.

All the plasmids constructed and used in this study are listed in Table S2. Mini-CRISPR element consisting of two repeats flanking the PAM-protospacer was synthesized by BGI (Shenzhen, China). PCR was performed using the iProof™ High-Fidelity DNA Polymerase (Bio-Rad, USA). Mini-CRISPR elements and plasmid pAY5211 were digested using the restriction enzymes KpnI and BamHI (NEB, USA) and ligated using the Quick Ligation Kit (NEB, USA) to generate the targeting plasmid. Donor sequences which typically contain 500-bp upstream and 500-bp downstream of the editing sites were amplified by PCR and ligated into the linearized targeting plasmid (digested by XhoI (NEB, USA)) using the ClonExpress One Step Cloning Kit (Vazyme, China). All the constructed plasmids were verified by DNA sequencing (BGI, China).

Transformation of PA154197.

Electrocompetent PA154197 cells were prepared by firstly innoculoating a fresh colony in LB broth and grown at 37°C overnight with 220-rpm agitation. Following subculture into 50 ml fresh LB broth and growing to OD_{600} = 0.5, cells were collected by centrifugation and washed three times with cold autoclaved Milli-Q H_2O. The resulting cells were resuspended into 1 ml Milli-Q H_2O. 100 μl electrocompetent PA154197 cells were then mixed with 1 μg editing plasmid and subject to electroporation (BTX, USA). 1 ml cold LB broth was added to recover the cells. Following culturing at 37°C for 1 h with agitation, cells were pelleted and resuspended in 100 μl

410 LB for spreading (LB+KAN500). Transformants colonies were obtained after incubation at 37°C
411 for 16-20 h.
412
413 **Mutant screening and verification.**
414 Colonies were firstly subjected to luminescence screening using the Synergy HTX Plate Reader
415 (Bio Tek, USA). Colonies with high luminescent intensity were further verified by colony PCR
416 using Taq DNA polymerase (Thermal Scientific, USA) with indicated primers and DNA
417 sequencing (BGI, China). Sequencing results were visualized using DNA sequencing software
418 Chromas (Technelysium Pty Ltd, Australia)
419
420 **Curing of editing plasmid.**
421 *P. aeruginosa* cells underwent one round of editing was streaked onto the LB ager plate and
422 incubated at 37°C overnight. Single colony was selected and the curing was verified by the failure
423 of growth in LB with 100 μg/ml KAN.
424
425 **Minimum inhibitory concentration (MIC) measurement.**
426 MIC was measured following the standard protocol of ASM with slight modification (52). A single
427 fresh colony of PA154197 was inoculated in LB medium overnight at 37°C with agitation.
428 Overnight culture was then diluted to cell density of 10^5/ml, and 200 μl of the cells were distributed
429 to each well of the 96-well plate. Antibiotics were then added with final concentrations ranging
430 from 0.25 to 128 μg/ml. Plates were incubated at 37°C for 16-20 h and MIC value was determined
431 by absorbance at 600 nm.
432

Reverse transcription (RT)-quantitative PCR (qPCR).

Bacterial cells from overnight culture were harvested by centrifugation at 4°C. Total RNA was extracted using RNeasy Mini Kit (Qiagen, Germany) according to the manufacturer's instruction. Reverse transcription was performed using PrimeScript RT reagent Kit (Takara, Japan). qPCR was performed using specific primers and the SYBR Green PCR master mix (Applied Biosystems, USA) in a 20 µl reaction system. The reaction was performed in ABI StepOnePlus real time PCR system with *recA* and *clpX* as reference genes to normalize the relative expression of the target genes. The results were expressed as fold change of the expression of target genes, and results were presented as the mean of three independent biological isolates.

Disk diffusion assay.

20 µl overnight culture as described above was mixed with 5 ml melted LB top agar (0.75 %) and poured on an LB agar plate. After the agar was solidified, round filter paper disks were placed. 5µl antibiotic solution (2 mg/ml) was added to the center of the paper disks. The plates were incubated at 37°C for 16 h.

ACKNOWLEDGEMENT

We thank Prof. Patrick CY Woo (Department of Microbiology, The University of Hong Kong) for providing the clinical PA isolates and Prof. Susumu Yoshizawa and Prof. Kazuhiro Kogure (Both from the University of Tokyo) for sharing the ocean-100 strain. We appreciate Dr. Xin Deng (Department of Biomedical Sciences, City University of Hong Kong) for the pMS402 vector.

This work was supported by the Hong Kong University Grants Council General Research Fund (HKU17142316 to A.Y.), Seed Funding for Basic Research Scheme of The University of Hong Kong (201711159278 to A.Y.), Seed Funding for Strategic Interdisciplinary Research Scheme (HKU 2017 to A.Y.), and National Natural Science Foundation of China (No. 31571283 to H.X.).

Z.X., M.L., H.X. and A.Y. designed research; Z.X. and Y.L. performed experiments; H.C. contributed to the bioinformatic analysis; Z.X., M.L., H.X. and A.Y. analysed data, wrote and revised the manuscript.

The authors do not have conflict of interests to declare.

REFERENCES

1. Oliver A, Mulet X, López-Causapé C, Juan C. 2015. The increasing threat of *Pseudomonas aeruginosa* high-risk clones. Drug Resist Updates 21:41-59.

2. Stover CK, Pham XQ, Erwin A, Mizoguchi S, Warrener P, Hickey M, Brinkman F, Hufnagle W, Kowalik D, Lagrou M. 2000. Complete genome sequence of *Pseudomonas aeruginosa* PAO1, an opportunistic pathogen. Nature 406:959-964.

3. Poole K. 2011. *Pseudomonas aeruginosa*: resistance to the max. Front Microbiol 2:65.

476 4. Santajit S, Indrawattana N. 2016. Mechanisms of antimicrobial resistance in ESKAPE
477 pathogens. BioMed Res Int 2016:2475067.

478 5. Magiorakos AP, Srinivasan A, Carey R, Carmeli Y, Falagas M, Giske C, Harbarth S, Hindler
479 J, Kahlmeter G, Olsson-Liljequist B. 2012. Multidrug-resistant, extensively drug-resistant
480 and pandrug-resistant bacteria: an international expert proposal for interim standard
481 definitions for acquired resistance. Clin Microbiol Infect 18:268-281.

482 6. Hocquet D, Berthelot P, Roussel-Delvallez M, Favre R, Jeannot K, Bajolet O, Marty N,
483 Grattard F, Mariani-Kurkdjian P, Bingen E, Husson MO, Couetdic G, Plesiat P. 2007.
484 *Pseudomonas aeruginosa* may accumulate drug resistance mechanisms without losing its
485 ability to cause bloodstream infections. Antimicrob Agents Chemother 51:3531-3536.

486 7. Cabot G, Ocampo-Sosa AA, Dominguez MA, Gago JF, Juan C, Tubau F, Rodriguez C, Moya
487 B, Pena C, Martinez-Martinez L, Oliver A, Spanish Network for Research in Infectious D.
488 2012. Genetic markers of widespread extensively drug-resistant *Pseudomonas aeruginosa*
489 high-risk clones. Antimicrob Agents Chemother 56:6349-6357.

490 8. Hocquet D, Bertrand X, Kohler T, Talon D, Plesiat P. 2003. Genetic and phenotypic
491 variations of a resistant *Pseudomonas aeruginosa* epidemic clone. Antimicrob Agents
492 Chemother 47:1887-1894.

493 9. Köhler T, Epp SF, Curty LK, Pechère J-C. 1999. Characterization of MexT, the regulator of
494 the MexE-MexF-OprN multidrug efflux system of *Pseudomonas aeruginosa*. J Bacteriol
495 181:6300-6305.

10. Bruchmann S, Dötsch A, Nouri B, Chaberny IF, Häussler S. 2012. Quantitative contribution of target alteration and decreased drug accumulation to *Pseudomonas aeruginosa* fluoroquinolone resistance. Antimicrob Agents Chemother 57:1361-1368.

11. Riera E, Cabot G, Mulet X, Garcia-Castillo M, del Campo R, Juan C, Canton R, Oliver A. 2011. *Pseudomonas aeruginosa* carbapenem resistance mechanisms in Spain: impact on the activity of imipenem, meropenem and doripenem. J Antimicrob Chemother 66:2022-2027.

12. Llanes C, Hocquet D, Vogne C, Benali-Baitich D, Neuwirth C, Plesiat P. 2004. Clinical strains of *Pseudomonas aeruginosa* overproducing MexAB-OprM and MexXY efflux pumps simultaneously. Antimicrob Agents Chemother 48:1797-1802.

13. Horna G, Lopez M, Guerra H, Saenz Y, Ruiz J. 2018. Interplay between MexAB-OprM and MexEF-OprN in clinical isolates of *Pseudomonas aeruginosa*. Sci Rep 8:16463.

14. Li XZ, Plesiat P, Nikaido H. 2015. The challenge of efflux-mediated antibiotic resistance in Gram-negative bacteria. Clin Microbiol Rev 28:337-418.

15. Lee A, Mao WM, Warren MS, Mistry A, Hoshino K, Okumura R, Ishida H, Lomovskaya O. 2000. Interplay between efflux pumps may provide either additive or multiplicative effects on drug resistance. J Bacteriol 182:3142-3150.

16. Vogwill T, Kojadinovic M, MacLean RC. 2016. Epistasis between antibiotic resistance mutations and genetic background shape the fitness effect of resistance across species of *Pseudomonas*. Proc R Soc B 283:20160151.

17. de Sousa JM, Balbontín R, Durão P, Gordo IJPb. 2017. Multidrug-resistant bacteria compensate for the epistasis between resistances. PLoS Biol 15:e2001741.

517 18. Vogwill T, Kojadinovic M, Furio V, MacLean RC. 2014. Testing the role of genetic
518 background in parallel evolution using the comparative experimental evolution of antibiotic
519 resistance. Mol Biol Evol 31:3314-3323.

520 19. van Belkum A, Soriaga LB, LaFave MC, Akella S, Veyrieras J-B, Barbu EM, Shortridge D,
521 Blanc B, Hannum G, Zambardi G. 2015. Phylogenetic distribution of CRISPR-Cas systems
522 in antibiotic-resistant *Pseudomonas aeruginosa*. MBio 6:e01796-15.

523 20. Cheng F, Gong L, Zhao D, Yang H, Zhou J, Li M, Xiang H. 2017. Harnessing the native type
524 IB CRISPR-Cas for genome editing in a polyploid archaeon. J Genet Genomics 44:541-548.

525 21. Zhang J, Zong W, Hong W, Zhang Z-T, Wang Y. 2018. Exploiting endogenous CRISPR-Cas
526 system for multiplex genome editing in *Clostridium tyrobutyricum* and engineer the strain for
527 high-level butanol production. Metab Eng 47:49-59.

528 22. Li Y, Pan S, Zhang Y, Ren M, Feng M, Peng N, Chen L, Liang YX, She Q. 2015. Harnessing
529 Type I and Type III CRISPR-Cas systems for genome editing. Nucleic Acids Res 44:e34-e34.

530 23. Pyne ME, Bruder MR, Moo-Young M, Chung DA, Chou CP. 2016. Harnessing heterologous
531 and endogenous CRISPR-Cas machineries for efficient markerless genome editing in
532 *Clostridium*. Sci Rep 6: 25666.

533 24. Cao H, Xia T, Li Y, Xu Z, Bougouffa S, Lo YK, Bajic VB, Luo H, Woo PC, Yan A. 2018. A
534 multidrug resistant clinical *P. aeruginosa* isolate in the MLST550 clonal complex: uncoupled
535 quorum sensing modulates the interplay of virulence and resistance. bioRxiv
536 https://doi.org/10.1101/415000.

537 25. Yonezawa M, Takahata M, Matsubara N, Watanabe Y, Narita H. 1995. DNA gyrase *gyrA*
538 mutations in quinolone-resistant clinical isolates of *Pseudomonas aeruginosa*. Antimicrob
539 Agents Chemother 39:1970-1972.

540 26. Juan C, Maciá MD, Gutiérrez O, Vidal C, Pérez JL, Oliver A. 2005. Molecular mechanisms
541 of β-lactam resistance mediated by AmpC hyperproduction in *Pseudomonas aeruginosa*
542 clinical strains. Antimicrob Agents Chemother 49:4733-4738.

543 27. Richter C, Gristwood T, Clulow JS, Fineran PC. 2012. In vivo protein interactions and
544 complex formation in the *Pectobacterium atrosepticum* subtype IF CRISPR/Cas System.
545 PLoS One 7:e49549.

546 28. Cady KC, Bondy-Denomy J, Heussler GE, Davidson AR, O'Toole GA. 2012. The
547 CRISPR/Cas adaptive immune system of *Pseudomonas aeruginosa* mediates resistance to
548 naturally occurring and engineered phages. J Bacteriol 194:5728-5738.

549 29. Leenay RT, Beisel CL. 2017. Deciphering, communicating, and engineering the CRISPR
550 PAM. J Mol Biol 429:177-191.

551 30. Olsen RH, DeBusscher G, McCombie WR. 1982. Development of broad-host-range vectors
552 and gene banks: self-cloning of the *Pseudomonas aeruginosa* PAO chromosome. J Bacteriol
553 150:60-69.

554 31. Shah NC. 2014. PhD Thesis. University of Hertfordshire, Hatfield, Hertfordshire, UK.
555 Construction and development of bioluminescent *Pseudomonas aeruginosa* strains;
556 application in biosensors for preservative efficacy testing.

557 32. Xu L, Chen H, Hu XH, Zhang RM, Zhang Z, Luo ZW. 2006. Average gene length is highly
558 conserved in prokaryotes and eukaryotes and diverges only between the two kingdoms. Mol
559 Biol Evol 23:1107-1108.

560 33. Chen W, Zhang Y, Zhang Y, Pi Y, Gu T, Song L, Wang Y, Ji Q. 2018. CRISPR/Cas9-based
561 genome editing in *Pseudomonas aeruginosa* and cytidine deaminase-mediated base editing
562 in *Pseudomonas* species. iScience 6:222-231.

563 34. Chen W, Zhang Y, Yeo W-S, Bae T, Ji Q. 2017. Rapid and efficient genome editing in
564 *Staphylococcus aureus* by using an engineered CRISPR/Cas9 system. J Am Chem Soc
565 139:3790-3795.

566 35. Kumagai Y, Yoshizawa S, Nakamura K, Ogura Y, Hayashi T, Kogure K. 2017. Complete
567 and Draft Genome Sequences of Eight Oceanic *Pseudomonas aeruginosa* Strains. Genome
568 Announc 5:e01255-17.

569 36. Köhler T, Michéa-Hamzehpour M, Henze U, Gotoh N, Kocjancic Curty L, Pechère JC. 1997.
570 Characterization of MexE–MexF–OprN, a positively regulated multidrug efflux system of
571 *Pseudomonas aeruginosa.* Mol Microbiol 23:345-354.

572 37. Sánchez P, Rojo F, Martínez JL. 2002. Transcriptional regulation of *mexR*, the repressor of
573 *Pseudomonas aeruginosa mexAB-oprM* multidrug efflux pump. FEMS Microbiol Lett
574 207:63-68.

575 38. Adewoye L, Sutherland A, Srikumar R, Poole K. 2002. The *mexR* repressor of the *mexAB-*
576 *oprM* multidrug efflux operon in *Pseudomonas aeruginosa*: characterization of mutations
577 compromising activity. J Bacteriol 184:4308-4312.

578 39. Saito K, Yoneyama H, Nakae T. 1999. *nalB*-type mutations causing the overexpression of
579 the MexAB-OprM efflux pump are located in the *mexR* gene of the *Pseudomonas aeruginosa*
580 chromosome. FEMS Microbiol Lett 179:67-72.

581 40. Maseda H, Saito K, Nakajima A, Nakae T. 2000. Variation of the *mexT* gene, a regulator of
582 the MexEF-oprN efflux pump expression in wild-type strains of *Pseudomonas aeruginosa*.
583 FEMS Microbiol Lett 192:107-112.

584 41. Linares JF, López JA, Camafeita E, Albar JP, Rojo F, Martínez JLJJob. 2005. Overexpression
585 of the multidrug efflux pumps MexCD-OprJ and MexEF-OprN is associated with a reduction
586 of type III secretion in Pseudomonas aeruginosa. J Bacteriol 187:1384-1391.

587 42. Quale J, Bratu S, Gupta J, Landman D. 2006. Interplay of efflux system, *ampC*, and *oprD*
588 expression in carbapenem resistance of *Pseudomonas aeruginosa* clinical isolates.
589 Antimicrob Agents Chemother 50:1633-1641.

590 43. Köhler T, Michea-Hamzehpour M, Epp SF, Pechere J-C. 1999. Carbapenem activities against
591 *Pseudomonas aeruginosa*: respective contributions of OprD and efflux systems. Antimicrob
592 Agents Chemother 43:424-427.

593 44. Varughese LR, Rajpoot M, Goyal S, Mehra R, Chhokar V, Beniwal V. 2018. Analytical
594 profiling of mutations in quinolone resistance determining region of gyrA gene among UPEC.
595 PloS one 13:e0190729.

596 45. Tretter EM, Berger JM. 2012. Mechanisms for Defining Supercoiling Set Point of DNA
597 Gyrase Orthologs I. A NONCONSERVED ACIDIC C-TERMINAL TAIL MODULATES
598 *ESCHERICHIA COLI* GYRASE ACTIVITY. J Biol Chem 287:18636-18644.

599 46. Breidenstein EB, de la Fuente-Núñez C, Hancock RE. 2011. *Pseudomonas aeruginosa*: all
600 roads lead to resistance. Trends Microbiol 19:419-426.

601 47. Cheng VC, Wong SC, Ho P-L, Yuen K-Y. 2016. Strategic measures for the control of surging
602 antimicrobial resistance in Hong Kong and mainland of China. Emerg Microbes Infect 4:e8.

603 48. Wright GD. 2016. Antibiotic adjuvants: rescuing antibiotics from resistance. Trends
604 Microbiol 24:862-871.

605 49. Jia B, Raphenya AR, Alcock B, Waglechner N, Guo P, Tsang KK, Lago BA, Dave BM,
606 Pereira S, Sharma AN. 2016. CARD 2017: expansion and model-centric curation of the
607 comprehensive antibiotic resistance database. Nucleic Acids Res 45(D1):D566-D573.

608 50. Choi K-H, Schweizer HP. 2005. An improved method for rapid generation of unmarked
609 *Pseudomonas aeruginosa* deletion mutants. BMC Microbiol 5:30.

610 51. Sun J, Deng Z, Yan A. 2014. Bacterial multidrug efflux pumps: mechanisms, physiology and
611 pharmacological exploitations. Biochem Biophys Res Commun 453:254-267.

612 52. Lalitha M. 2004. Manual on antimicrobial susceptibility testing. Performance standards for
613 antimicrobial testing: Twelfth Informational Supplement 56238:454-456.

614

615

FIGURE AND TABLE LEGENDS

FIG 1 Repurposing the functional native CRISPR-Cas system for gene deletion. (A) Schematic representation of the native type I-F CRISPR-Cas in PA154197. Diamonds and rectangles indicate the repeat and spacer units of a CRISPR array, respectively. Curved arrows (in black) above the leader sequence (in brown) indicate the orientation of CRISPR transcription. The consensus repeat of the two CRISPR arrays differs by one nucleotide (in red). **(B)** Schematic showing the design of the *mexB*-targeting plasmid (pAY5233) and the *mexB*-deletion donor. The mini-CRISPR in pAY5233 comprises a 32-bp spacer (in blue) targeting the *mexB* gene and two flanking repeats (in yellow), and is co-expressed with the reporter *lux* operon (in green) under the control of the strong promoter P*tat*. The PAM sequence is framed. The donor (in pink) consists of sequences upstream (U1) and downstream (D1) of *mexB*. The *Kpn*I and *BamH*I sites are used for mini-CRISPR insertion and the *Xho*I site is used for one-step cloning of the donor. **(C)** Representative plates showing the transformation efficiency of the vector control pAY5211, the targeting plasmid pAY5233, and the editing plasmid pAY5235. **(D)** Design of the *mexB*-deletion plasmid pAY5235 which contains both the self-targeting CRISPR and the repair donor. **(E)** Eight randomly selected transformants were subjected to colony PCR to screen for the Δ*mexB* mutants (positive clones are highlighted in red). Primers used in colony PCR (F1/R1) are indicated in panel (B). **(F)** The screened Δ*mexB* mutants in (E) were further validated by DNA sequencing.

FIG 2 Expression levels of the *mexAB*, *mexEF* and *oprD* genes in PAO1, PA154197 and its isogenic mutants *mexR*^{PAO1}, *mexT*^{PAO1}. (A) Schematic showing the regulation of *mexAB-oprM*, *mexEF-oprN* and *oprD* in *P. aeruginosa*. MexR represses the expression of *mexAB-oprM*; MexT activates *mexEF-oprN* and represses *oprD*. **(B&C)** Transcription alteration of *mexA* and *mexB* in

PA154197 and in PAO1, and in PA154197 and its isogenic *mexR*^{PAO1} mutant. Transcription of *mexF* in the two strains serves as a negative control whose expression is not affected by MexR. **(D&E)** Transcription alteration of *mexE*, *mexF* and *oprD* in PA154197 and in PAO1, and in PA154197 and its isogenic *mexT*^{PAO1} mutant. Transcription of *mexA* in the two strains serves as a negative control whose expression is not affected by MexT.

FIG 3 The two-step In-Del editing strategy (taking insertion of 8 bp into *mexT* as an example). **(A)** Schematic design of the two-step In-Del method. In the first step, a 32-bp exogenous DNA sequence (tag, in pink) is introduced to an auxiliary target site (in blue), between its PAM and protospacer portions. In the second step, a tag-targeting CRISPR, as well as a tag-lacking donor which contains the desired mutation (8-bp insertion in this case), is provided to simultaneously remove the exogenous tag and achieve the desired mutation. **(B)** Randomly selected luminescence positive colonies from the two steps were subjected to colony PCR using the primers F3/Seq-R3 (indicated in panel **A**). Desired mutants are highlighted in red. **(C)** Targets in the potential mutants from the two steps were amplified using the primers Seq-F3/Seq-R3 (indicated in panel **A**) and validated by DNA sequencing. Representative DNA sequencing results from the two steps are shown, where the tag sequence is shown in pink.

FIG 4 Substrate scheme of the MexAB-OprM and MexEF-OprN efflux systems. Substrate profiles of the MexAB-OprM and MexEF-OprN and their preferences are shown schematically based on the MIC alterations (Table 1 and 2) in the Δ*mexB*, Δ*mexF*, Δ*mexB* Δ*mexF* and *gyrA*^{PAO1} *mexT*^{PAO1} *mexR*^{PAO1} cells relative to the WT. The greater the MIC changes in the single mutant relative to the WT, the stronger substrates they are denoted. The strength of the substrate

662 preference is expressed by the color key shown, except for the CHL, NAL and TMP (in grey)
663 which MICs were only changed in double or triple mutants.

664
665 **FIG 5 Schematic diagram of the native type I-F CRISPR-Cas mediated genome editing in**
666 **PA154197 and its exploitations in functional genomics investigation.** Desired mutants with
667 altered resistance (or virulence, other physiology) can be obtained in one step by introducing a
668 programmable editing plasmid, which carries a mini-CRISPR (expressing a crRNA) and a repair
669 donor, into the MDR/XDR PA154197 cells with ready luminescence selection. The crRNA directs
670 the Cascade complex to the target. Recombination occurs between the repair donor and the target
671 area to prevent the target interference, resulting in the desired mutation. Two-step editing can be
672 utilized to obtain mutations in the genetic loci that cannot be well targeted by CRISPR. A red
673 asterisk indicates a resistant determinant in PA154197. Cells containing the editing plasmid
674 expressing the *lux* genes are shown in light green.

675
676 **Table 1**. MICs (μg/ml) of various antipseudomonal antibiotics in PAO1, PA154197 and its isogenic
677 mutants

678
679 **Table 2.** MICs (μg/ml) of various antibiotics and antimicrobial agents in PAO1, PA154197 and its
680 isogenic mutants

681

682 **FIGURE AND TABLE LEGENDS FOR SUPPLEMENTAL MATERIALS**

683 **FIG S1 Effect of desired truncation lengths on the efficiency of editing. (A)** Schematic diagram
684 of the genetic locus of *mexB* and adjacent region. Desired truncation fragments of 50 bp (B1, 74-

123), 500 bp (B2, 74-573), 1000 bp (B3, 74-1073), the full length (*mexB*, 1-3141), and the primers to test these truncations are shown. **(B)** Positive clones of each of truncations in eight randomly selected transformants are highlighted in red.

FIG S2 Curing of the editing plasmid in the edited cells. Edited cells could not grow in the presence of kanamycin (100 μg/ml) after plasmid curing, which was achieved by culturing the edited cells without antibiotic pressure overnight.

FIG S3 Harnessing the native type I-F CRISPR-Cas system for genome editing in other *P. aeruginosa* isolates. The single editing plasmid pAY5235 was transformed in the clinical *P. aeruginosa* isolate PA150567 and the environmental isolate Ocean-100 to achieve *mexB* deletion in one-step. Eight randomly selected luminescent transformants were subjected to colony PCR to screen for the desired Δ*mexB* mutants. Positive clones are highlighted in red. Primers used in colony PCR are indicated in Figure 1B.

FIG S4 Disk diffusion assay of the antibiotic susceptibilities of PA154197 and its isogenic mutants. Disk diffusion test is conducted to examine the susceptibility of PA154197 and its isogenic mutants to eight antipseudomonal drugs **(A)** and six other antibiotics and antimicrobial agents **(B)**. Larger inhibition zone represents the higher susceptibility to the indicated antibiotics.

FIG S5 Growth curves of PA154197 and its isogenic mutants in the absence of antibiotics. No difference of growth among PA154197 and its isogenic mutants were observed.

FIG S6 Comparative genomics reveals mutations in the key antibiotic resistance genes *mexR*, *mexT* and GyrA in PA154197. (A) The point mutation (G226T) in PA154197 *mexR* gene leads to premature termination of its protein product. **(B)** An 8-bp deletion in PA154197 *mexT* relative to that in PAO1 converts the out-of-frame *mexT* product to the in-frame, active form of *mexT* product. **(C)** PA154197 *gyrA* gene contains a T248C substitution (corresponding to T83I in the GyrA protein) in the quinolone resistance-determining region (QRDR) and a ^{2723}CCGAGT^{2728} 6-bp deletion (corresponding to the deletion of E959&S960) in the C terminal domain of the gene product.

FIG S7 Non-efficient targeting at the desired editing site in the *mexT* gene. (A) Schematic showing the desired 8-bp insertion (CGGCCAGC) into the *mexT* gene. The 6-bp repeat sequences (in red) in the target which potentially obscure the targeting by the CRISPR-Cas apparatus are shown. PAM is shown in frame. **(B)** No desirable DNA interference was observed by transforming the *mexT*-targeting plasmid pAY5900 into PA154197 cells in comparison with the control plasmid pAY5211. Note that no repair donor was provided in this plasmid.

FIG S8 Replacing the essential gene *gyrA* with that from PAO1 using the two-step In-Del method. (A) Schematic showing the two-step strategy for *gyrA* gene replacement. The tag sequence (in pink) is first introduced downstream of *gyrA* (in orange) between the PAM and protospacer portions of a selected target (in blue). In the second step, a tag-targeting plasmid carrying the repair donor (Del-donor) is provided. Del-donor lacks the tag sequence but contains the *gyrA* gene (in dark blue) from PAO1, which is flanked by two ~1000-bp sequences upstream and downstream of the PA154197 *gyrA* gene. The primer pairs F/Seq-R and Seq-F/Seq-R were

731 used for the colony PCR analysis in (B) and DNA sequencing, respectively. **(B)** Eight luminescent
732 positive transformants from each editing step were randomly selected for colony PCR analysis.
733 Desired mutants confirmed by DNA sequencing are highlighted in red.
734
735 **Table S1.** A summary of mutational changes in the antibiotic resistance (AR) genes in PA154197
736 by comparative genomic analysis
737
738 **Table S2.** Bacterial strains, plasmids used in this study
739

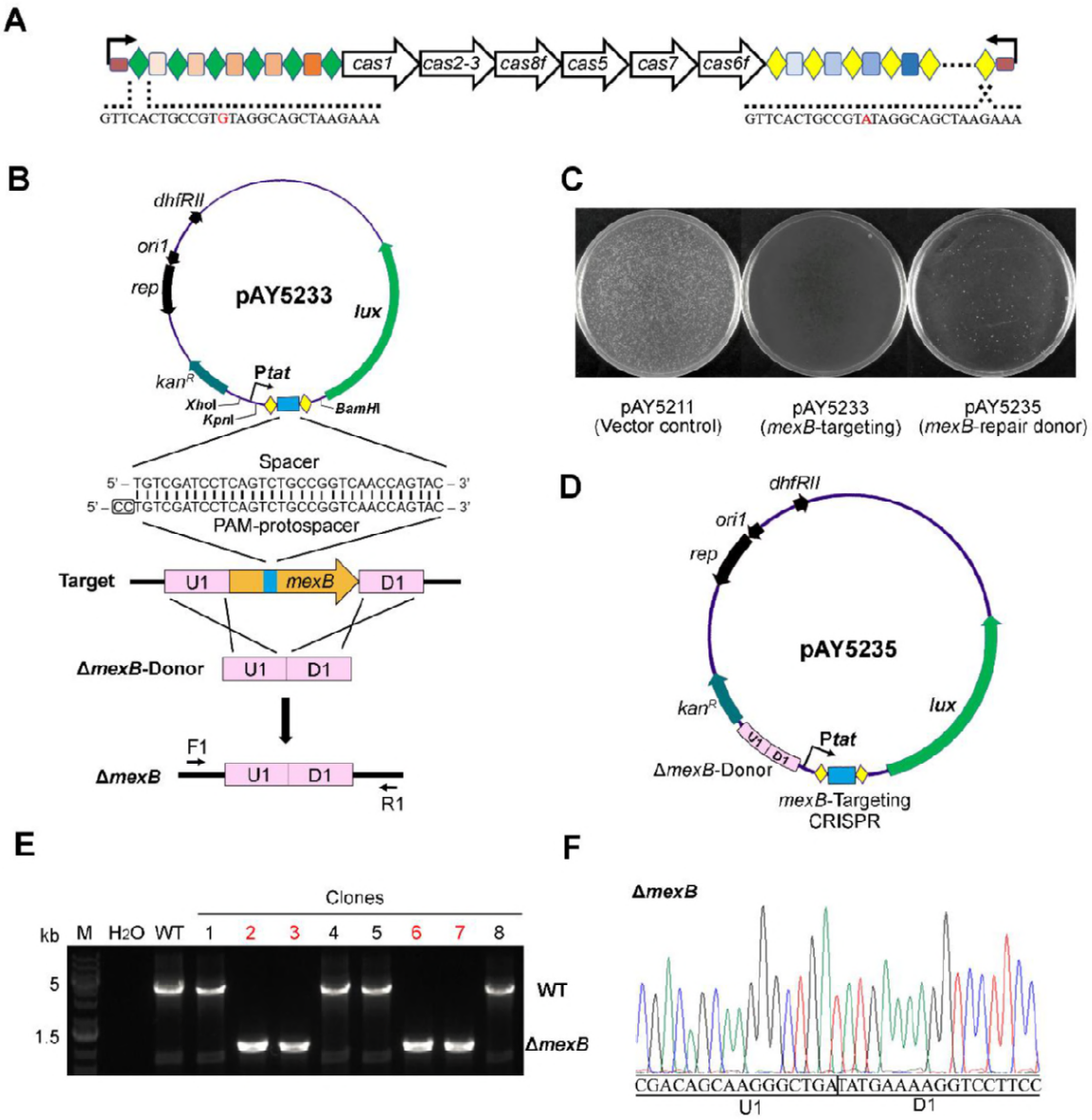

FIG 1 Repurposing the functional native CRISPR-Cas system for gene deletion. (A) Schematic representation of the native type I-F CRISPR-Cas in PA154197. Diamonds and rectangles indicate the repeat and spacer units of a CRISPR array, respectively. Curved arrows (in black) above the leader sequence (in brown) indicate the orientation of CRISPR transcription. The consensus repeat of the two CRISPR arrays differs by one

nucleotide (in red). **(B)** Schematic showing the design of the *mexB*-targeting plasmid (pAY5233) and the *mexB*-deletion donor. The mini-CRISPR in pAY5233 comprises a 32-bp spacer (in blue) targeting the *mexB* gene and two flanking repeats (in yellow), and is co-expressed with the reporter *lux* operon (in green) under the control of the strong promoter P*tat*. The PAM sequence is framed. The donor (in pink) consists of sequences upstream (U1) and downstream (D1) of *mexB*. The *Kpn*I and *BamH*I sites are used for mini-CRISPR insertion and the *Xho*I site is used for one-step cloning of the donor. **(C)** Representative plates showing the transformation efficiency of the vector control pAY5211, the targeting plasmid pAY5233, and the editing plasmid pAY5235. **(D)** Design of the *mexB*-deletion plasmid pAY5235 which contains both the self-targeting CRISPR and the repair donor. **(E)** Eight randomly selected transformants were subjected to colony PCR to screen for the Δ*mexB* mutants (positive clones are highlighted in red). Primers used in colony PCR (F1/R1) are indicated in panel (B). **(F)** The screened Δ*mexB* mutants in (E) were further validated by DNA sequencing.

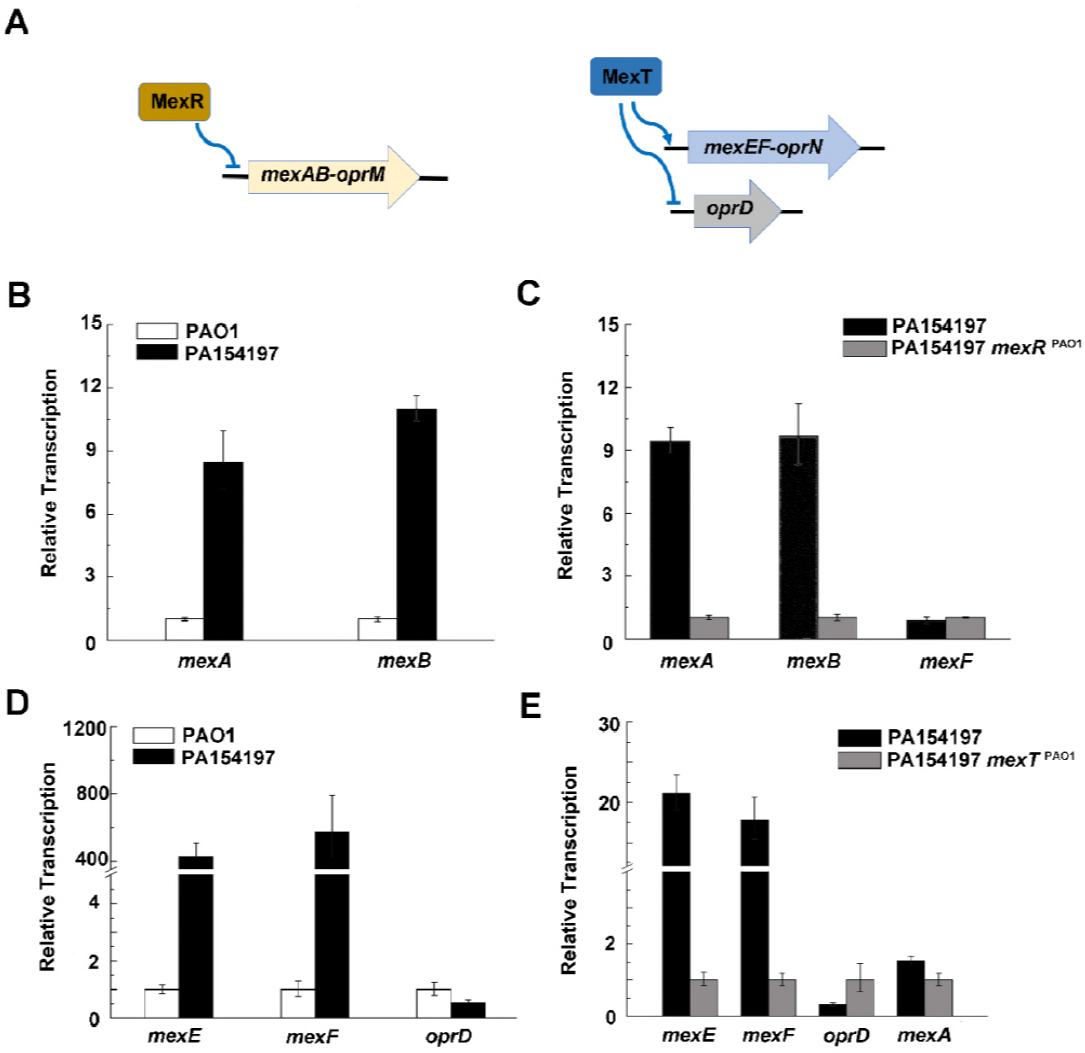

FIG 2 Expression levels of the *mexAB*, *mexEF* and *oprD* genes in PAO1, PA154197 and its isogenic mutants *mexR*^{PAO1}, *mexT*^{PAO1}. (A) Schematic showing the regulation of *mexAB-oprM*, *mexEF-oprN* and *oprD* in *P. aeruginosa*. MexR represses the expression of *mexAB-oprM*; MexT activates *mexEF-oprN* and represses *oprD*. **(B&C)** Transcription alteration of *mexA* and *mexB* in PA154197 and in PAO1, and in PA154197 and its isogenic *mexR*^{PAO1} mutant. Transcription of *mexF* in the two strains serves as a negative control whose expression is not affected by MexR. **(D&E)** Transcription alteration of

mexE, mexF and *oprD* in PA154197 and in PAO1, and in PA154197 and its isogenic *mexT*^{PAO1} mutant. Transcription of *mexA* in the two strains serves as a negative control whose expression is not affected by MexT.

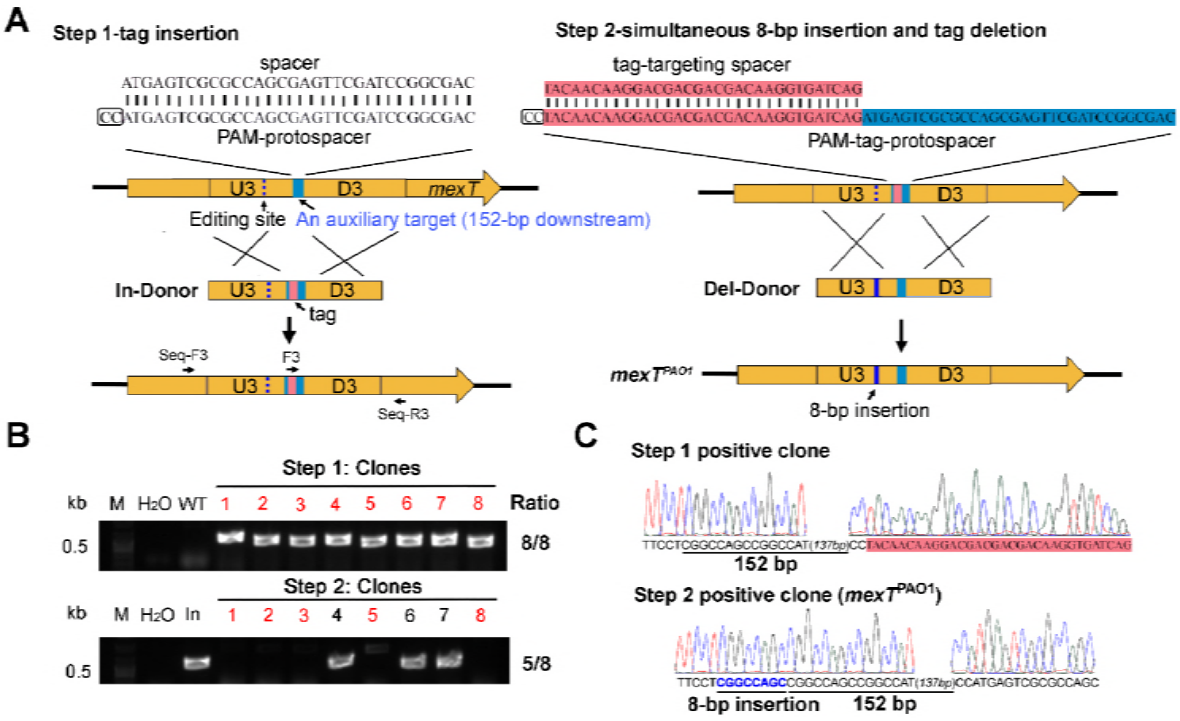

FIG 3 The two-step In-Del editing strategy (taking insertion of 8 bp into *mexT* as an example). (A) Schematic design of the two-step In-Del method. In the first step, a 32-bp exogenous DNA sequence (tag, in pink) is introduced to an auxiliary target site (in blue), between its PAM and protospacer portions. In the second step, a tag-targeting CRISPR, as well as a tag-lacking donor which contains the desired mutation (8-bp insertion in this case), is provided to simultaneously remove the exogenous tag and achieve the desired mutation. **(B)** Randomly selected luminescence positive colonies from the two steps were subjected to colony PCR using the primers F3/Seq-R3 (indicated in panel **A**). Desired mutants are highlighted in red. **(C)** Targets in the potential mutants from the two steps were amplified using the primers Seq-F3/Seq-R3 (indicated in panel **A**) and validated by

DNA sequencing. Representative DNA sequencing results from the two steps are shown, where the tag sequence is shown in pink.

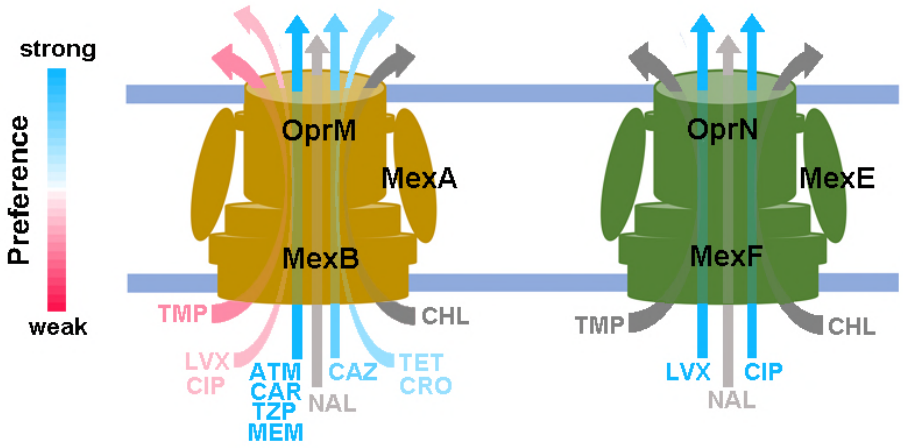

FIG 4 Substrate scheme of the MexAB-OprM and MexEF-OprN efflux systems. Substrate profiles of the MexAB-OprM and MexEF-OprN and their preferences are shown schematically based on the MIC alterations (Table 1 and 2) in the Δ*mexB*, Δ*mexF*, Δ*mexB* Δ*mexF* and *gyrA*^{PAO1} *mexT*^{PAO1} *mexR*^{PAO1} cells relative to the WT. The greater the MIC changes in the single mutant relative to the WT, the stronger substrates they are denoted. The strength of the substrate preference is expressed by the color key shown, except for the CHL, NAL and TMP (in grey) which MICs were only changed in double or triple mutants.

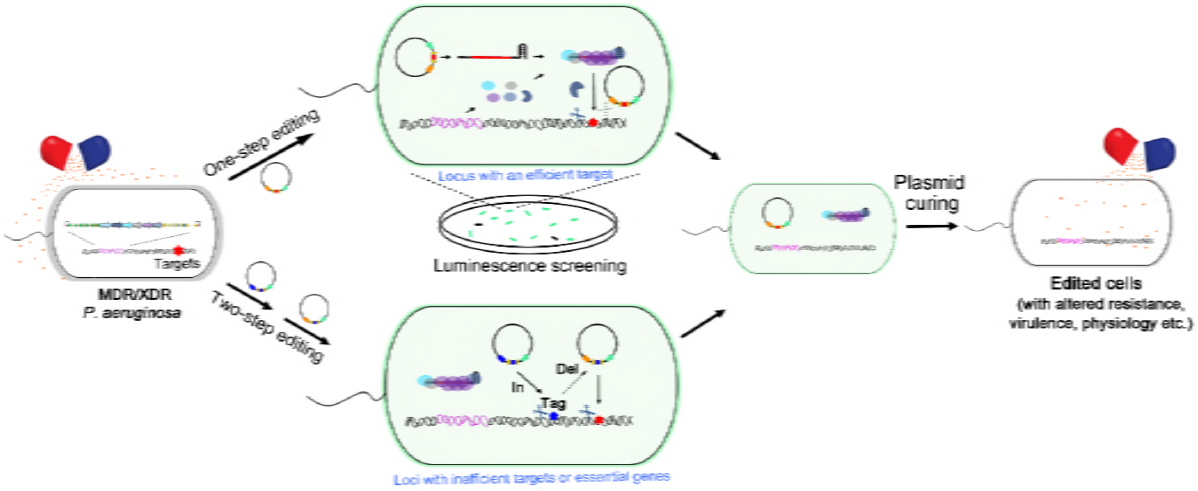

FIG 5 Schematic diagram of the native type I-F CRISPR-Cas mediated genome editing in PA154197 and its exploitations in functional genomics investigation. Desired mutants with altered resistance (or virulence, other physiology) can be obtained in one step by introducing a programmable editing plasmid, which carries a mini-CRISPR (expressing a crRNA) and a repair donor, into the MDR/XDR PA154197 cells with ready luminescence selection. The crRNA directs the Cascade complex to the target. Recombination occurs between the repair donor and the target area to prevent the target interference, resulting in the desired mutation. Two-step editing can be utilized to obtain mutations in the genetic loci that cannot be well targeted by CRISPR. A red asterisk indicates a resistant determinant in PA154197. Cells containing the editing plasmid expressing the *lux* genes are shown in light green.

Table 1. MICs (μg/ml) of various antipseudomonal antibiotics in PAO1, PA154197 and its isogenic mutants

Strains	**ATM**	**CAZ**	**TZP**	**MEM**	**CAR**	**LVX**	**CIP**	**IPM**
PAO1	4	1	2	0.5	32	0.25	0.25	2
PA154197	**64**	**16**	**32**	**4**	**>128**	**32**	**16**	**4**
Mutations lead to increased drug susceptibilities:								
Δ*mexB*	**1** (1/64)	**2** (1/8)	**0.5** (1/64)	**<0.125**	**1** (1/128)	**16** (1/2)	**8** (1/2)	4
Δ*mexF*	64	16	32	4	>128	**16** (1/2)	**4** (1/4)	4
Δ*mexB* Δ*mexF*	**0.5** (1/128)	**2** (1/8)	**0.5** (1/64)	**<0.125**	**1** (1/128)	**1** (1/32)	**0.5** (1/32)	4
mexR ^{PAO1}	**4** (1/16)	**4** (1/4)	**4** (1/4)	**0.5** (1/8)	**64** (1/2)	**16** (1/2)	**8** (1/2)	4
mexT ^{PAO1}	64	16	32	4	>128	**16** (1/2)	**4** (1/4)	**2** (1/2)
mexR ^{PAO1} *mexT* ^{PAO1}	**4** (1/16)	**4** (1/4)	**4** (1/4)	**0.25** (1/16)	**64** (1/2)	**2** (1/16)	**0.5** (1/32)	**2** (1/2)
gyrA ^{PAO1}	64	16	32	4	>128	**2** (1/16)	**4** (1/4)	4
gyrA ^{PAO1} *mexR* ^{PAO1}	**4** (1/16)	**4** (1/4)	**4** (1/4)	**0.5** (1/8)	**64** (1/2)	**2** (1/16)	**0.5** (1/32)	4
gyrA ^{PAO1} *mexT* ^{PAO1}	32	16	32	4	>128	**2** (1/16)	**0.5** (1/32)	**2** (1/2)
gyrA ^{PAO1} *mexR* ^{PAO1} *mexT* ^{PAO1}	**4** (1/16)	**4** (1/4)	**4** (1/4)	**0.25** (1/16)	**64** (1/2)	**0.25** (1/128)	**<0.125** (1/128)	**2** (1/2)
Mutations do not lead to increased drug susceptibilities:								
Δ*mexH*	64	16	32	4	>128	32	16	4
parS ^{PAO1}	64	16	32	4	>128	32	16	4

ATM: Aztreonam; **CAZ**: Ceftazidime; **TZP**: piperacillin-tazobactam; **MEM**: Meropenem; **CAR**: Carbenicillin; **LVX**: Levofloxacin; **CIP**: Ciprofloxacin; **IPM**: Imipenem

Table 2. MICs (μg/ml) of various antibiotics and antimicrobial agents in PAO1, PA154197 and its isogenic mutants

Strains	**NAL**	**TMP**	**CRO**	**TET**	**CHL**	**SDS**
PAO1	32	32	4	8	32	>128
PA154197	**>128**	**128**	**64**	**32**	**>128**	>128
Mutations lead to increased drug susceptibilities:						
Δ*mexB*	>128	**64** (1/2)	**16** (1/4)	**8** (1/4)	>128	>128
Δ*mexF*	>128	128	64	32	>128	>128
Δ*mexB* Δ*mexF*	>128	**4** (1/32)	**8** (1/8)	**4** (1/8)	**4** (1/32)	>128
mexR ^{PAO1}	>128	**64** (1/2)	**8** (1/8)	**8** (1/4)	>128	>128
mexT ^{PAO1}	>128	128	64	32	>128	>128
mexR ^{PAO1} *mexT* ^{PAO1}	>128	**32** (1/4)	**8** (1/8)	**8** (1/4)	**16** (1/8)	>128
gyrA ^{PAO1}	>128	128	64	32	>128	>128
gyrA ^{PAO1} *mexR* ^{PAO1}	>128	**64** (1/2)	**8** (1/8)	**8** (1/4)	>128	>128
gyrA ^{PAO1} *mexT* ^{PAO1}	>128	128	64	32	>128	>128
gyrA ^{PAO1} *mexR* ^{PAO1} *mexT* ^{PAO1}	**32** (1/4)	**32** (1/4)	**8** (1/8)	**8** (1/4)	**16** (1/8)	>128
Mutations do not lead to increased drug susceptibilities:						
Δ*mexH*	>128	128	64	32	>128	>128
parS ^{PAO1}	>128	128	64	32	>128	>128

NAL: Nalidixic acid; **TMP**: Trimethoprim; **CRO**: Ceftriaxone; **TET**: Tetracycline; **CHL**: Chloramphenicol; **SDS**: Sodium dodecyl sulfate